energies

MDPI

Article

Inverse Properties Estimation of Methanol Adsorption in Activated Carbon to Utilise in Adsorption Cooling Applications: An Experimental and Numerical Study

Maaed Ossman [1], Majid Siavashi [1,*] and Masoud Babaei [2,*]

[1] Applied Multi-Phase Fluid Dynamic Laboratory, School of Mechanical Engineering, Iran University of Science and Technology, Tehran P.O. Box 16846-13114, Iran; maaed_ossman@mecheng.iust.ac.ir
[2] Department of Chemical Engineering, The University of Manchester, Manchester M13 9PL, UK
* Correspondence: msiavashi@iust.ac.ir (M.S.); masoud.babaei@manchester.ac.uk (M.B.)

Abstract: The precise estimation of influential parameters in adsorption is a key point in conducting simulations for the sensitivity analysis and optimal design of cooling systems. This study explores the critical role of a new type of granular activated carbon (GAC-208C) in adsorption refrigeration systems. By fitting experimental and numerical models to the thermophysical properties of GAC/methanol as a working pair, an advanced methodology is established for the thermal analysis of the adsorption bed, addressing the various operating conditions overlooked in prior studies. The physical properties of the studied carbon sample are determined in a laboratory using surface area and pore volume tests, thermal adsorption analysis, and weight loss. To determine the thermal properties of GAC/methanol, the adsorption process is experimentally tested inside an isolated heat exchanger. A three-dimensional (3D) model is created to simulate the procedure and then coupled with the particle swarm optimisation (PSO) algorithm in MATLAB. The optimal thermal parameters for adsorption are determined by minimising the mean square error (MSE) of the adsorption bed temperature between the numerical and experimental data. The laboratory studies yielded accurate results for the physical properties of GAC, including adsorption capacity, porosity, permeability, specific heat capacity, density, activation energy, and the heat of adsorption. The thermal analysis of the adsorption process identified the ideal values for the Dubinin–Astakhov equation constants, diffusion coefficients, heat transfer coefficients, and contact resistance. The numerical model demonstrated strong agreement with the experimental results, and the dynamic behaviour of pressure and uptake distribution showed good agreement with 1.2% relative error. This research study contributes to the improved estimation of adsorption parameters to conduct more accurate numerical simulations and design new adsorption systems with enhanced performance under different operating conditions.

Keywords: adsorption cooling; thermophysical properties; inverse parameter estimation; granular activated carbon (GAC); experimental; numerical

Academic Editor: John Abraham

Received: 16 December 2024
Revised: 19 January 2025
Accepted: 30 January 2025
Published: 4 February 2025

Citation: Ossman, M.; Siavashi, M.; Babaei, M. Inverse Properties Estimation of Methanol Adsorption in Activated Carbon to Utilise in Adsorption Cooling Applications: An Experimental and Numerical Study. *Energies* **2025**, *18*, 714. https://doi.org/10.3390/en18030714

1. Introduction

Recent research has predominantly concentrated on the practical applications of adsorption refrigeration systems, driven by the contemporary industrial revolution that seeks innovative industrial technologies utilising alternative energy sources to address the continual rise in greenhouse gas emissions [1,2]. These systems employ a variety of adsorbent–adsorbate combinations, such as activated carbon with methanol, ethanol,

ammonia, silica gel and zeolite with water [3]. The thermophysical properties of each pair are pertinent to appropriate refrigeration applications, including air conditioning, water desalination, and heat pumps [4]. The critical physical parameters of adsorbent materials include porosity, permeability, the heat of adsorption, specific heat capacity, and activation energy [5]. Alongside the adsorption equation coefficients, thermal diffusion coefficients, effective heat transfer coefficients, and contact resistance, these properties define the total physical thermal characteristics that govern the adsorption process, which varies depending on the working pair [6].

The examination of the thermal performance and cooling capacity of adsorption systems has garnered significant attention lately [7], which renders assessing the sensitivity of these parameters critically important in this research. Based on the specified characteristics of the working pair, certain equations are used to examine the dynamics and kinetics of adsorption [8,9]. Conducting reliable thermodynamic studies and achieving reasonable cooling performance depends on accurately knowing these parameters. Most studies have focused solely on the parameters of the adsorption heat equation or the physical properties of the adsorbent material [10] while neglecting the importance of determining the kinetic parameters of adsorption. This has necessitated repeating tests of the thermophysical properties of current adsorption systems under various conditions [11]. Wang et al. [12] tested activated carbon (AC) using methanol, ethanol, and ammonia coolants for refrigeration purposes. The specific heat capacity, density, average thermal conductivity, adsorption capacity, and constants of the Dubinin–Astakhuv (D-A) equation were determined by creating a testing unit (AC/methanol). The methods used to obtain these characteristics were not clearly defined. The study by Rupam et al. [13] on carbon adsorption using experimental and numerical methods showed significant variations in the values of isothermal heat and adsorption capacity, confirming that many properties of the working pairs suffer from inaccuracies in their precise determination. Wu et al. [14] evaluated the adsorption properties of three types of activated carbon. It is noteworthy that in a different study conducted by Yagnamurthy et al. [15] on a specific type of Maxsorb III carbon, using the same analysis and similar conditions for the adsorption analysis equation (D-A), different ranges for the same properties were estimated, showing that these results are inaccurate. Zhao et al. [16] examined the (D-A), Langmuir, and Freundlich models for three types of AC. It was found that the (D-A) model is the most sensitive one for determining the adsorption coefficients. In addition to these models, Rahman et al. [17] proposed other optimisation models for adsorption isotherms and stated that the T'oth model is the most suitable one for specific pairs, such as silica gels. Also, in investigations to improve the cooling system's performance, the thermal conductivity of the working fluid in porous media (λ) and the contact resistance (h_{Res}) with the adsorption bed wall was examined [4,18]. In this context, Jegede and Critoph [19] developed the thermal jump technique to derive these properties by measuring the temperature of the adsorption bed at intervals across a predetermined range, with root mean square deviation (RMSD $\pm$ 5%). In a study by Khaliji Oskouei and Tamainot-Telto [20] on the temperature fluctuations of the adsorption tube during desorption, thermal conductivity and contact resistance for granular activated carbon (GAC) samples with varied densities were determined. Since heat conductivity and contact resistance must be calculated using the relevant equations for adsorption dynamics, these methods are still under study.

Even though GAC is being studied in adsorption refrigeration cycles, its thermophysical properties as a working pair in its adsorption equations have not been fully characterised. Conversely, the majority of assessments have relied on repeated constants despite their varying experimental conditions [3,21]. Also, the use of advanced equation models for computational fluid dynamics analysis is crucial to ensure the uniform distri-

bution of temperature, pressure, and uptake inside the adsorption bed. However, most previous studies have lacked advanced analyses in this area, particularly when it comes to using simplified linear equations for specific directions within the adsorption bed [22]. In a study by Shabir et al. [8] on the AC207EA carbon type with methanol, the constants of the Dubinin–Astakhov equation were completely different from those values presented by Hassan et al. [9] while utilising identical analytical equations and experimental conditions. Elsheniti et al. [23] provided some parameters for the AC/ethanol pair, such as permeability, porosity, exponential constant, the heat of adsorption, and thermal conductivity, but the method of obtaining these parameters was unclear, particularly for a 3-D model. Moreover, recent research has focused on silica gel and zeolite pairs with water for desalination by using advanced equation models for computational fluid dynamics analysis [24]. Mohammed et al. [5] tested silica/water adsorption kinetic models, such as the linear driving force (LDF), Darcy's law, and heat and mass transfer. However, the equations of these models use constant and iterative parameters, resulting in more than 10% deviations. Mitra et al. [25] studied how ethanol vapour moved through the carbon adsorption bed and how it changed the temperature, pressure, and uptake distribution in different ranges. However, the distribution did not include the integration of all the equations needed for a 3-D dynamic analysis of the adsorption bed under specified boundary conditions. Previous analyses, as well as many other studies on the evaluation of adsorption processes [26], have shown that data related to thermophysical properties are repeated over large ranges despite the fact that these processes operate under different conditions, resulting in unacceptable errors in performance indicator estimates.

This has prompted current research to investigate the discrepancies between experimental results and numerical data when estimating adsorption parameters in order to reduce these errors by developing new techniques to link adsorption equation models, resulting in a qualitative leap in the modernisation of adsorption refrigeration systems. Accordingly, this research study uses a new type of domestically produced GAC-208C with distinctive properties that make it suitable for use in adsorption refrigeration systems. This study first determines physical properties through laboratory tests, including adsorption capacity, activation energy, specific heat capacity, density, porosity, permeability, and the heat of adsorption. The physical parameters are inputs for a 3D adsorption bed model that is operated using AC/methanol to estimate the thermal parameters. The model is implemented in COMSOL Multiphysics software Version 6.2 and simulates the experimental adsorption process within a heat exchanger. This approach involves linking this model to the particle swarm optimisation (PSO) algorithm in MATLAB to minimise the mean square error (MSE) between experimental and numerical temperature data at the bed centre. The optimal values for the adsorption equation parameters (including diffusion coefficients, effective heat transfer coefficient, and contact resistance) are determined using the inverse parameter estimation method. The procedure is validated by finding the relative error of the experimental pressure and uptake for the new properties. As a result, the total error is 0.87%, which shows high reliability for the proposed model.

2. Materials and Experimental Procedures

Activated carbon is one of the most widely used materials in adsorption refrigeration cycles. If the cooling system is adequately examined, it creates an appropriate working pair to achieve good thermal performance [27]. Activated carbon comes from a variety of sources, including walnut and peach shells [8]. Therefore, there are many types of extraction, depending on the source and technique of extraction, such as powder, granular, fibre, and many other types [9].

The current study is based on special tests to evaluate the properties of (208C) granular activated carbon, manufactured by pyrolysis and carbonisation processes of cellulosic materials in coconut shells, which is produced by the Shimi Pajoohan Company in Iran, Tehran with a (8 × 30) US sieve mesh size (0.6 × 2.36 mm), which is equivalent to an average diameter of 3.2×10^{-4} [m]. Figure 1 depicts several forms of AC as well as the granular carbon sample on which the appropriate tests are carried out.

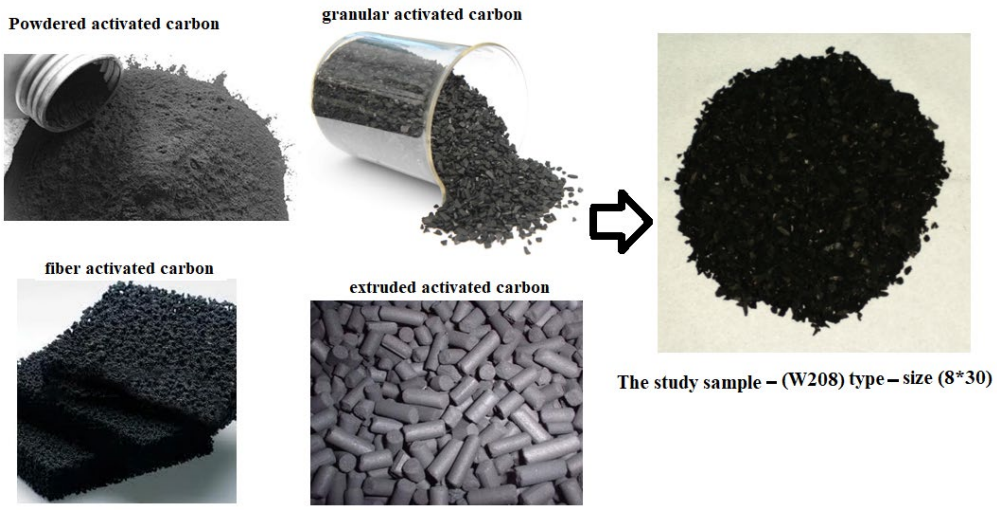

Figure 1. The granular activated carbon sample of type 208C and size 8 × 30.

This study includes two rounds of tests, one in the laboratory to evaluate the physical properties of AC independently, and the other is a setup to identify the main parameters of the AC/methanol working pair during the adsorption process. The second test is carried out after introducing the parameters collected from the first test. We will present a summary of these experiments, which will assist in demonstrating an appropriate technique to estimate the relevant parameters of the adsorption equations.

2.1. Laboratory Thermal Tests

Thermal tests, such as the Brunauer–Emmett–Teller (BET) test, are used to assess the essential features of the activated carbon sample [28]. It is used to analyse adsorption by measuring the specific surface area, density, and porosity using a high-precision device, as shown in Figure 2a. At different temperatures, the adsorption of nitrogen into the AC sample is examined, and the adsorbed gas volume is calculated as a function of the relative pressure [13,14].

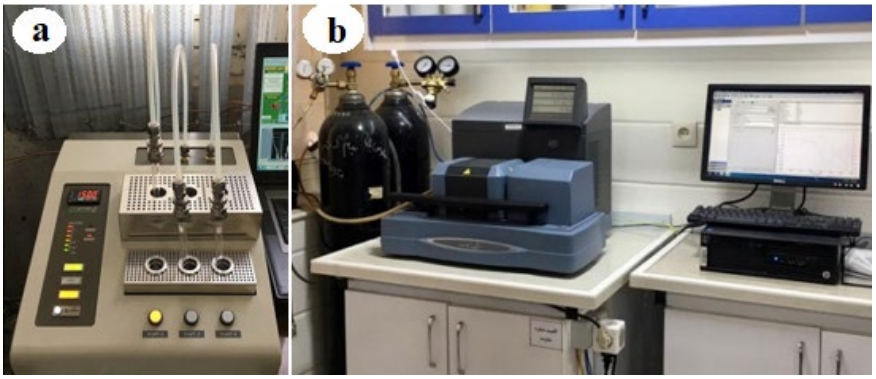

Figure 2. Estimating the thermal properties of the activated carbon by (**a**) BET; and (**b**) DSC devices.

The specific heat capacity and adsorption enthalpy of the sample in different temperatures can be assessed using the differential scanning calorimetry (DSC) test [29], as shown in Figure 2b. Thus, the thermal behaviour of the energy difference according to thermocouples is drawn, allowing several physical parameters of the researched sample to be estimated at the corresponding temperatures.

Thermal gravimetric analysis (TGA) is another method of detecting changes in the mass of a sample as a result of a temperature rise, that is, the amount of weight loss due to the temperature increase [30]. If the TGA results are similar, distinguishing between them will not be easy. To remedy this issue, a curved derivative TGA shows the turning points as peaks in the so-called derived thermal gravimeter (DTG), allowing for a more precise examination of the material's behaviour under heat [31].

2.2. Methanol Adsorption in the Activated Carbon Test

The experimental work is separated into various steps, beginning with establishing the proper heat exchanger and its packing equipment, continuing with connecting the drying and cooling cycle of the AC, and concluding with the adsorption process, as follows:

2.2.1. Heat Exchanger and Measuring Equipment

Because the adsorption bed is the heart of the refrigeration system, its proper design allows heat and mass transfer inside the GAC porous bed, resulting in more efficient adsorption. Based on this importance, a customised heat exchanger is created for this experiment, consisting of a large tube housing the AC sample and a fine tube-shaped holder that allows the methanol liquid to enter and distribute uniformly within the carbon bed. Two tight-fitting caps are also at the top and bottom to prevent leakage. Figure 3 depicts a schematic shape, the constructed heat exchanger, and the necessary parts and measurement tools. The tube and its cylindrical holder are constructed of 316 stainless steel for storing the AC under precise heat conditions. One of the covers contains a central hole through which a tube holder with a diameter of 3 mm and a length of 200 mm is inserted and used to connect the thermocouple wire to the carbon bed's core.

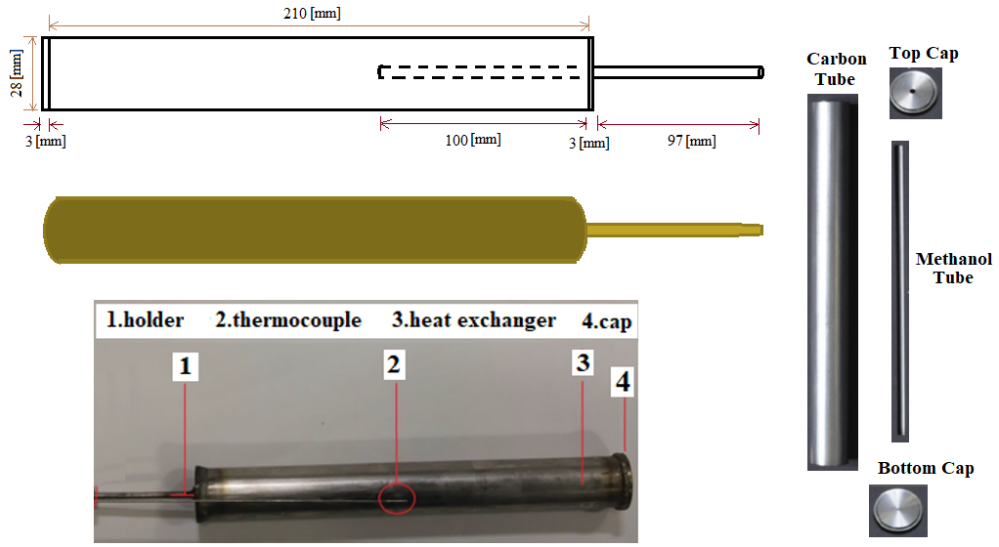

Figure 3. A schematic of the heat exchanger with geometric dimensions and structural parts.

Gradual loading is used to fill 26 g of GAC in numerous stages. The tube is immersed in water for several minutes to check that there is no air in the sample, and then it is ready as an adsorption bed to be connected to the rest of the equipment in the adsorption cycle. In the cycle, an electric heater is used to heat the heat exchanger for the drying process via

a furnace attached to it; a vacuum pump is used to empty the air cycle. Also, the methanol tank, a power supply (voltage regulator), and a data logger are on hand. Figure 4 depicts the schematic interface of the adsorption cycle.

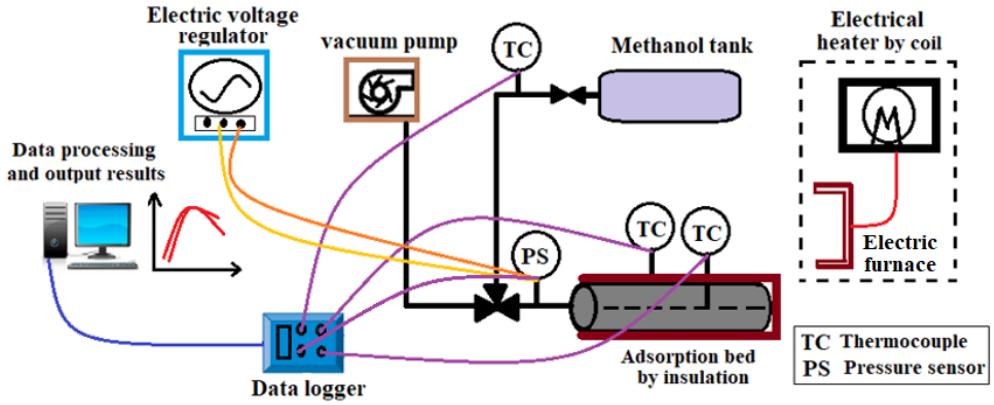

Figure 4. Diagram of the investigated adsorption cycle.

A digital scale is used to weigh the carbon sample, and a thermal camera monitors the thermal activities inside the adsorption bed. K-type thermocouples measure the temperature at the centre and wall points of the adsorption bed and transmit it to the data logger device. The pressure inside the heat exchanger is measured using an Edwards ASG1000-Druck (Eastbourne, UK) pressure sensor with a measurement range of 0 to 5 bar, a DC input of 7 to 32 [V], and an output current of 4 to 20 [mA], operating over the temperature range of 313 to 453 [K]. The Pico TC-08 gadget, which has eight channels, collects data from all linked devices, such as the thermocouples and pressure sensors; it is immediately connected to the laptop via the USB port, and the data are recorded every 5 s.

To correctly measure thermophysical properties, the cycle action must be organised, which requires employing more precise instruments. So, Table 1 shows the error percentage in the utilised equipment and tools.

Table 1. Errors in the measuring instruments used in the experiment.

Instrument	Thermocouple	Pressure Sensor	Power Supply	Sample Scale	Heater
Error	±0.1 [K]	±0.01 [Pa]	±0.001 [V]	±0.05 [g]	±0.01 [J]

2.2.2. Adsorption Process Test

The adsorption process necessitates removing moisture from the activated carbon at high temperatures, evacuating the work cycle from the air, and selecting suitable ambient conditions. Therefore, this procedure is divided into two stages:

In the drying cycle, the heat exchanger is exposed to a high temperature of 450 [K] for 6 h inside an electric oven. The drying process is monitored using K-type thermocouples placed inside the heat exchanger and on its walls in order to distribute heat uniformly across the carbon, along with a high-precision pressure sensor placed at the inlet of the heat exchanger. This heat treatment is carried out concurrently through the vacuum pump, which continuously evacuates the air, reducing the pressure to about 8–10 [kPa] and improving drying efficiency. Figure 5 shows the drying and air evacuation cycles.

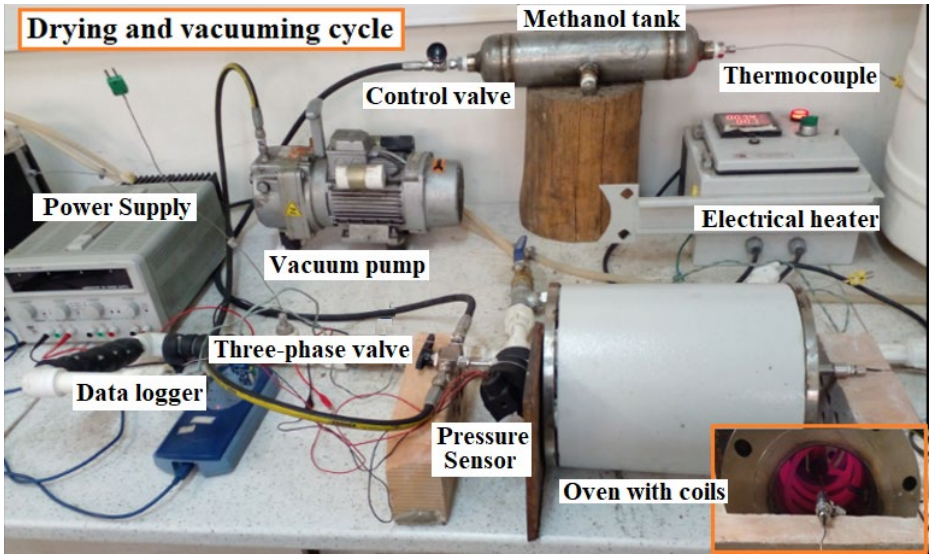

Figure 5. Drying carbon and removing air from the adsorption cycle.

After drying and evacuating air, the heat exchanger is left to be cooled to ambient temperature and then insulated by an elastomeric insulator with good insulation properties. After that, it is connected to the methanol tank via a three-way control valve after closing it from the side of the vacuum pump, as it is well controlled manually during the switching with continuous monitoring, although it operates under low pressures.

The adsorption process between methanol and activated carbon begins inside the heat exchanger, and the temperature inside the heat exchanger is monitored by a thermocouple connected to the centre of the adsorption bed (as exhibited in Figure 6). This cycle operates as an isolated dynamic system without any external thermal stimulus so that the setup allows the detailed monitoring of the adsorption kinetics based on the intrinsic properties of the AC/methanol pair.

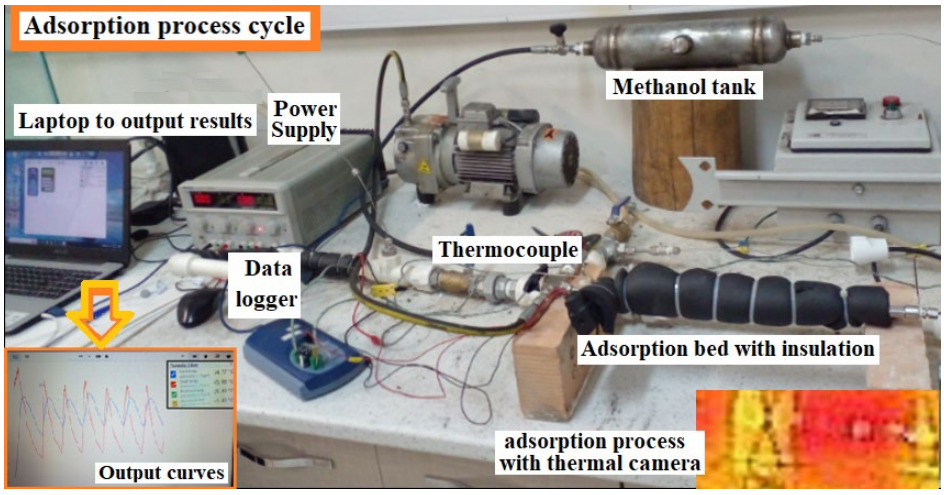

Figure 6. Adsorption process setup and recording data through a data logger on a computer.

The temperature changes inside the adsorption bed show a significant increase due to the exothermic nature of adsorption. The temperature changes within the range 295–303 [K], followed by a gradual stabilisation at the time of 3500 [s] for the end of the adsorption process. The laptop's PicoLog 6 software records data readings at regular intervals (50 s). The information collected within the data loggers is displayed in tabular values that are saved within the software. These values are taken from a thermocouple

directly connected to the centre of the adsorption bed. The setup is repeated several times, allowing the continuous and accurate monitoring of the adsorption kinetics. The adsorption bed is weighed with a weight balance to calculate the decrease in uptake between 0.5 and 0.2 kg⁄kg. Additionally, pressure readings are taken by a pressure sensor at the inlet of the adsorption bed, 1100–1104 [Pa], in the same way and at time intervals.

In each iteration of the adsorption process, the insulator is removed upon drying and reinserted upon the initiation of the adsorption process. The cycle pressure is well monitored to ensure the stability of the adsorption process and the absence of any leakage problems. Repeating the experiment under different operating conditions ensures that the adsorption behaviour is consistent with theoretical models and also provides valuable insights into the performance of the AC/methanol.

3. Modelling of the Adsorption Process

The adsorption refrigeration cycle operates in four stages (heating, adsorption, cooling, and desorption), according to the Clapeyron diagram [22]. However, what encouraged us to analyse the unknown adsorption and thermal parameters through heat and mass transfer in porous media [21] is that these parameters of the working pair material directly affect the adsorption process performance [7].

The 3D experimental heat exchanger is represented by a 2D axisymmetric numerical model, as shown in Figure 7. The unknown parameters are estimated using an inverse procedure to fit the numerical results on the experimental data.

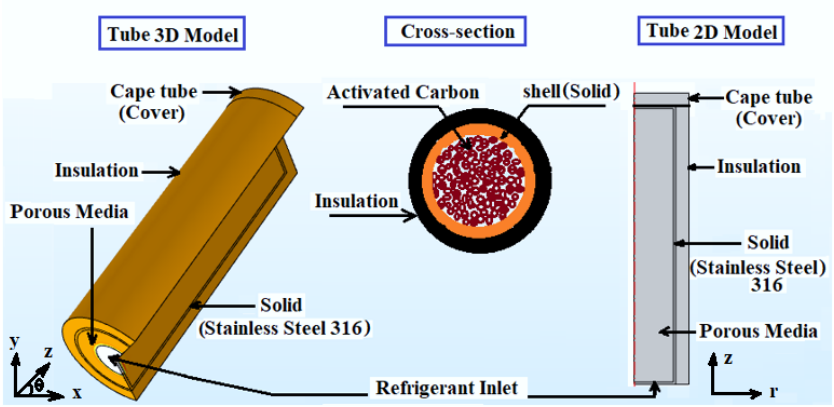

Figure 7. The 3D experimental model and the 2D numerical representation.

Table 2 shows the thermophysical properties of the materials used in the experiment. Table 3 displays the initial and boundary conditions involving temperatures, pressure, and initial uptake. Such data are used in the numerical simulation after experimental validation by using thermocouple, pressure sensor and thermoflow devices to measure the temperatures, pressures and fluid velocity of the adsorption bed inlets and environment of the laboratory, then repeating this for several consecutive days.

Table 2. Thermophysical properties of adsorption bed installations.

Physical Property	ρ [kg/m^3]	$C_{p,s}$ [J/(kg.K)]	λ [W/(m.K)]	$C_{p,v}$ [J/(kg.K)]	μ [kg/(m.s)]
Methanol	791	2530	0.55	2200	1×10^{-5}
Stainless Steel	8700	460	80	----------	----------
Elastomeric Thermal Insulation	55	1200	0.055	----------	----------

Table 3. Initial and boundary conditions for simulating the adsorption process.

Initial and Boundary Conditions	T_{eva} [K]	T_{amb} [K]	P_{eva} [kPa]	V_{meth} [m/s]	X_{ini} [kg/kg]	T_{in} [K]
Values of the adsorption bed	291	294	1.1	0.005	0	295

Due to the complexity of the adsorption process within porous media, some assumptions and simplifications are considered, which are listed as follows:

1. During adsorption, the AC/methanol working pair is in thermal equilibrium.
2. The permeability, porosity, viscosity, and contact resistance coefficients between particles are constant in a stable medium.
3. The gaseous state of the refrigerant follows ideal gas conditions.
4. The methanol flow is distributed constantly within the adsorption layer.

Based on these assumptions, the following mathematical and numerical models are used to simulate the adsorption process.

3.1. Mathematical Model

In this investigation, an initial estimation for the thermophysical properties of AC is determined using the equations of the curves resulting from its laboratory analysis.

3.1.1. Laboratory Tests Equations

The isothermal exit diagram for testing (BET) can be used to calculate porosity, permeability, adsorption capacity, and other properties, as shown in Figure 8 [28].

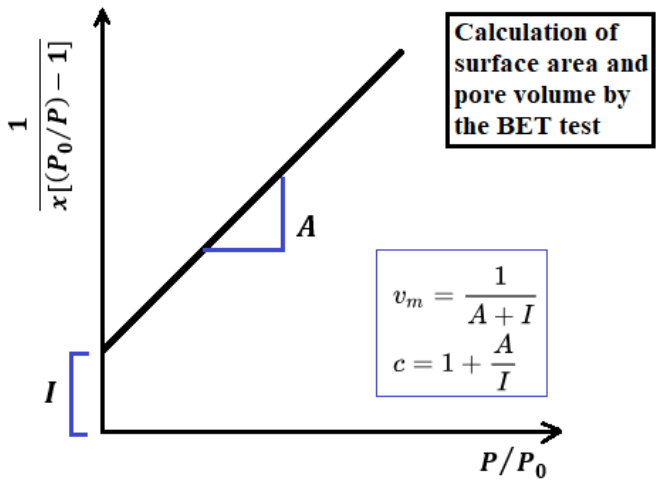

Figure 8. BET plot function for relative pressure.

Meanwhile, the BET equation is as follows [28]:

$$\frac{1}{x[(P_0/P)-1]} = \frac{c-1}{x_o.c}\left(\frac{P}{P_0}\right) + \frac{1}{x_o.c} \quad (1)$$

P: pressure of the adsorbed gas in the equilibrium state.
P_0: partial pressure of adsorbed gas [Pa].
v_a: volume of the adsorbed gas in standard conditions T = 273.15 [K], $P = 1.013 \times 10^5$ [Pa].

v_m: volume of the gas adsorbed in the standard state to produce a single layer on the sample's surface [mm^3], where , v_a, v_m are obtained from the BET test results of an activated carbon sample.

c: constant value that depends on the enthalpy of adsorption of the adsorbed gas on the powder sample. The value of parameter c is calculated based on the following relationship:

$$c = exp\left(\frac{E_1 - E_L}{RT}\right) \tag{2}$$

In this Equation, E_1 is the heat of adsorption to form the first single layer and E_L is the heat of adsorption to create the second layer. The constant value (c) varies according to the type of gas used.

Since the adsorbed refrigerant is placed between the adsorbent cavities, the maximum amount of refrigerant adsorption x_o is calculated by multiplying the specific volume of the adsorbent micropores (ν_s) by the density of the refrigerant liquid (ρ_l) at atmospheric pressure [32].

$$x_o = \rho_l \nu_s \tag{3}$$

The activated carbon sample will be tested to produce an adsorption curve (BET) that is proportional to the previous curve produced in a special laboratory. Thus, we can determine the physical properties extracted from it by taking advantage of the slope of the resulting curve and the previous equations. This can be found in detail in the results section.

The Arrhenius equation is used in the DSC and TGA tests for calculating the activation energy (E_a), which represents the amount of change in the heat flow as a consequence of the temperature change (β) at the test curve's peak points, as follows [31]:

$$\ln\left(\frac{\beta}{T^2}\right) = \ln\left(\frac{AR}{E_a}\right) + 0.61 - E_a/R \tag{4}$$

T, A, E, and R are the absolute temperature [K], pre-exponential factor [min^{-1}], apparent activation energy [$kJ.mol^{-1}$], and the gas constant [$J.mol^{-1}.K^{-1}$], respectively.

The remaining properties of the activated carbon are derived directly from the analysis of the resulting curves [30].

3.1.2. Adsorption Bed Equations

The energy equation in porous media contains three different states: solid, gas, and adsorbate. Because the study's goal is to reflect only the adsorption process, the term related to heat transferring fluid is ignored and replaced by the adsorption term associated with uptake changes as a function of the evaporation temperature of the refrigerant, as expressed as follows [26,33]:

$$\begin{aligned}(1-\varepsilon)\rho_{AC}C_{p.AC}\frac{\partial T_{AC}}{\partial t} + \varepsilon\rho_v C_{p.v}\frac{\partial T_{AC}}{\partial t} + (1-\varepsilon)\rho_{AC}xC_{p.l}\frac{\partial T_{AC}}{\partial t}\\ -(1-\varepsilon)\rho_{AC}|\Delta H_{ads}|\frac{\partial x}{\partial t} - \varepsilon\frac{\partial P}{\partial t} - \lambda_{AC}\nabla^2 T_{AC} + \rho_v C_{p.v}\boldsymbol{u}\nabla T_{AC}\\ +\rho_v C_{p.v}\frac{\partial x}{\partial t}(T_{eva} - T_{AC}) = 0\end{aligned} \tag{5}$$

($\Delta \boldsymbol{H_{ads}}$) represents the heat of adsorption, x is the adsorption capacity, and ε is the porosity of the adsorption bed. Also, ρ_{AC} and ρ_v are, respectively, the density of adsorbent material (AC) and refrigerant gas (methanol). T_{AC} is the adsorbent material temperature, ($\rho_{AC}C_{p.AC}$) is the total heat capacity of the adsorption bed, and $C_{p.AC}$ is the specific heat capacity of adsorbent material. $c_{p.v}$ and $c_{p.l}$, respectively, express the specific heat of

the refrigerant in the vapour and liquid phases.λ_{AC} represents the thermal conductivity coefficient of AC, $\boldsymbol{u}$ is the velocity vector of refrigerant gas vapour within the adsorbent bed, and T_{eva} is the evaporation temperature.

The refrigerant vapour density is calculated using the following relationship, which takes into account the refrigerant vapour in its ideal state [33]:

$$P = \rho_v R_V T_{AC} \tag{6}$$

Darcy's law for low gas velocities in porous media and both radial and axial directions can be used [34]:

$$u = -\frac{\kappa}{\mu}\frac{\partial P}{\partial r}; v = -\frac{\kappa}{\mu}\frac{\partial P}{\partial z} \tag{7}$$

where μ is the vapour viscosity, and the bed permeability (κ) is calculated by the semiempirical Blake–Kozeny equation [35,36]:

$$\kappa = \frac{d_p^2 \varepsilon^3}{150(1-\varepsilon)^2} \tag{8}$$

The mass conservation equation for the porous medium is as follows [10]:

$$\varepsilon\frac{\partial \rho_v}{\partial t} + (1-\varepsilon)\rho_{AC}\frac{\partial x}{\partial t} - D_m\nabla^2\rho_v + \nabla.(\boldsymbol{u}\rho_v) = 0 \tag{9}$$

The second and third terms, respectively, define the rate of adsorption and the diffusive mass transfer and D_m is the effective diffusion parameter.

The internal mass transfer resistance for the adsorption process is defined by the linear driving force (LDF) model [11,23]:

$$\frac{\partial x}{\partial t} = k_m(x_o - x) \tag{10}$$

where x represents the adsorbed amount and x_o is the equilibrium adsorption capacity of the adsorbent–adsorbate pair.

The internal mass transfer coefficient (k_m) is a measure of the flow of refrigerant vapour within the adsorbent particles [10] and is given by

$$k_m = \frac{15}{r_p^2} D_o \exp\left(-\frac{E_a}{RT_{AC}}\right) \tag{11}$$

where D_o is the pre-exponential constant of the surface diffusion or reference diffusivity, and r_p is the particle radius.

Through the previous relationship, we deduce the value of the effective diffusion parameter (D_m) as a function of the AC particle diameter or AC temperature according to two different formulas as follows [11,34]:

$$k_m = \frac{15}{r_p^2} D_m \text{ or } D_m = D_o \exp\left(-\frac{E_a}{RT_{AC}}\right) \tag{12}$$

The (D-A) equation used in the solution model is temperature-dependent [2,32]:

$$x = x_o exp[-D\left(\frac{T_{AC}}{T_{sat}} - 1\right)^n] \tag{13}$$

D is determined by the microstructure of the adsorbent, and (n) is the characteristic parameter of the adsorbent-adsorbed pair. In this regard, x_o, D and n are known as

Dubinin–Astakhov coefficients, and T_{sat} is the saturated temperature corresponding to the gas pressure, which is given according to Antoine's Equation [34]:

$$T_{sat} = 39.724 + \frac{1730.63}{8.07131 - \log_{10}(7.500638 \times 10^{-3} \times P)} \quad (14)$$

The contact resistance and external heat transfer coefficient of the adsorption bed are calculated by analysing the thermal resistances of its layers in the studied case (Model 2) and comparing them to the overall case (Model 1) as a function of the temperature distribution at each layer, as shown in Figure 9.

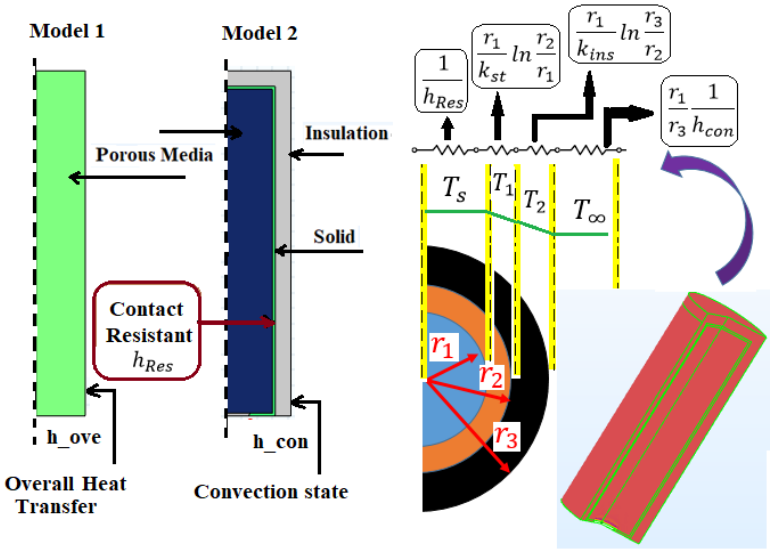

Figure 9. Thermal resistance distribution of the adsorption bed.

The amount of heat transferred between two points as a function of thermal resistance is given by the following relationship [37]:

$$q_r = \frac{T_s - T_\infty}{R_{tot}} \quad (15)$$

where (R_{tot}) is the total thermal resistance, which represents the layers of the heat exchanger, so the relationship becomes as follows:

$$q_r = \frac{T_s - T_\infty}{\frac{1}{2\pi r_1 L h_{Res}} + \frac{\ln(r_2/r_1)}{2\pi \lambda_{st} L} + \frac{\ln(r_3/r_2)}{2\pi \lambda_{ins} L} + \frac{1}{2\pi r_3 L \lambda_{con}}} \quad (16)$$

Thus, the overall heat transfer coefficient equation (Model 1) is as follows [37]:

$$U_{ove} = \frac{1}{\frac{1}{h_{Res}} + \frac{r_1}{\lambda_{st}} ln \frac{r_2}{r_1} + \frac{r_1}{\lambda_{ins}} ln \frac{r_3}{r_2} + \frac{r_1}{r_3} \frac{1}{\lambda_{con}}} \quad (17)$$

h_{Res} is the contact resistance between the porous medium and the wall of the adsorption bed, and h_{con} is the convective heat transfer coefficient for the outer layer.

The above equations are described in the physical section of the simulation model within the COMSOL software. The parameters of the equations are chosen as variable thermal properties according to the importance of their effect on the adsorption dynamics. The boundary conditions of these equations are chosen within a 3-D component that matches the conditions of the experimental work.

3.2. Numerical Model

The adsorption bed is investigated by using the 2D transient local thermal non-equilibrium (LTNE) model to study the adsorption of vapour within the adsorbent layers as a function of time. The simulation model is created by solving all of the mentioned governing equations with COMSOL Multiphysics software, which is based on the finite element method (FEM). The geometry is meshed using an extremely fine triangular mesh with 20,000 elements.

4. Inverse Parameter Estimation

The performance improvement of the adsorption bed depends on improving the heat and mass transfer model within it [38,39], which can only be achieved through properly selected design parameters. So, the physical properties of activated carbon calculated in the laboratory are entered into the simulation model by COMSOL, while the thermal properties are calculated through the inverse parameter estimation method by fitting the numerical results to the experimental data.

This method is defined by the numerical simulation of temperature variations at the centre of the adsorption bed and then fitting them to the experimental results of the adsorption process. The objective function is defined as the mean square error (MSE) between the experimental (T_{exp}) and the simulated (T_{sim}) results according to [20]:

$$\mathrm{MSE} = \frac{1}{N}\sum_{i=1}^{N}\left[\left(T_{exp}\right)_i - \left(T_{sim}\right)_i\right]^2 \tag{18}$$

where N is the total number of temperature samples (i). The particle swarm optimisation (PSO) algorithm within MATLAB R2022b software is implemented to minimise the above objective function [40], and the two software packages are linked via a special server [41]. Numerical simulations are carried out via COMSOL, and PSO estimates new parameters based on the simulation data. The estimation process begins by updating the selected parameters, followed by iterations at a variable population number, in order to achieve the best fit between the numerical and experimental temperature curves. The thermal parameters are tested within the longest range taken as previous reference values, while the optimal selection process is carried out in a distributed manner by this algorithm. Figure 10 depicts the flowchart of the estimation stages used to minimise the MSE objective function.

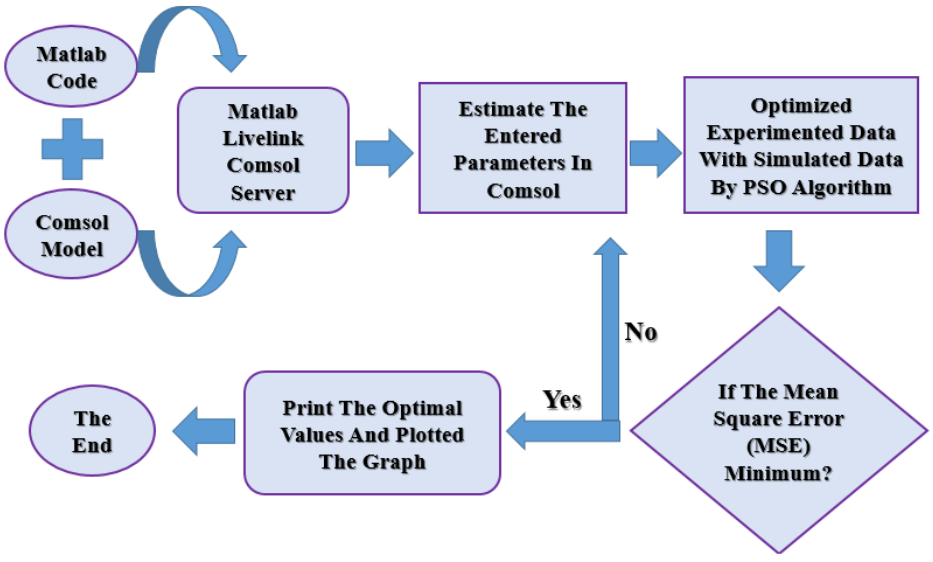

Figure 10. Flowchart of the inverse parameter estimation method.

Note that some inverse problems might be ill posed or have multiple solutions. Also, the inverse parameter estimation problems are sensitive to the initial guesses and might lead to nonphysical solutions. By employing this approach and utilising primary experimental data for parameter initialisation, we can effectively resolve this problem, thereby enhancing the accuracy and stability of the result. If a weak optimisation method is selected to perform inverse estimation, it is still likely to reach nonphysical solutions. By this method, we could minimise the error and chance of trapping the solution in nonphysical solutions.

5. Results and Discussion

The results are based on two groups, one focusing on detecting the properties of AC in the laboratory and the other on estimating the unknown parameters using the inverse method. After reaching suitable factors, the adsorption bed is tested to evaluate temperature, pressure, and uptake distribution.

5.1. Thermal Analysis Tests in the Laboratory

The BET test results provide detailed insights into the microscopic distribution of AC grains and quantify the specific surface area and total pore volume, which are critical for understanding the adsorption capacity and material efficiency. These parameters contribute to determining the amounts of porosity (ε) and permeability (k). All test results are directly displayed in Table 4, along with other parameters resulting from solving the previously described equations.

Table 4. BET test results of the activated carbon sample.

Activated Carbon Sample	BET Special Surface [m^2/g]	Total Pore Volume [cm^3/g]	BET Constant	Molar Volume [cm^3/g]	Maximum Adsorption [cm^3/g]	Volume Percentage of Micro-Holes [%]
208C (8 × 30)	938.79	0.5753	1341.7	215.69	374.9	42.1

The adsorption capacity (x_o) is estimated by the amount of vapour adsorbed inside the pores during the adsorption process, indicating the highest vapour value at a relative pressure (99%).

The results of the BET test are used to characterise the parameters of the adsorption equation produced using the two procedures. In the first situation (normal experimental), as shown in Figure 11a, the total pore volume is estimated employing the curve deviation angle with relative pressure changes, and the final calculation is performed using the experimental constant of nitrogen gas as defined in Equation (1). In the other procedure, which illustrates the adsorption/desorption processes in Figure 11b, the adsorbed gas volume is obtained as a function of relative pressure changes that reach the highest value (99%). As a result, the adsorption capacity could be determined using Equation (3).

According to the above, the BET analysis reveals the specific surface area and total pore volume of the activated carbon, which are two key factors in determining its adsorption capacity. A high specific surface area indicates adsorption sites that enhance the ability of this type of carbon to adsorb methanol, while the total pore volume provides insight into the storage capacity of this type. Both cases impact the speed and efficiency of methanol molecules' adsorption into the carbon matrix, thereby influencing the overall performance of the refrigeration cycle.

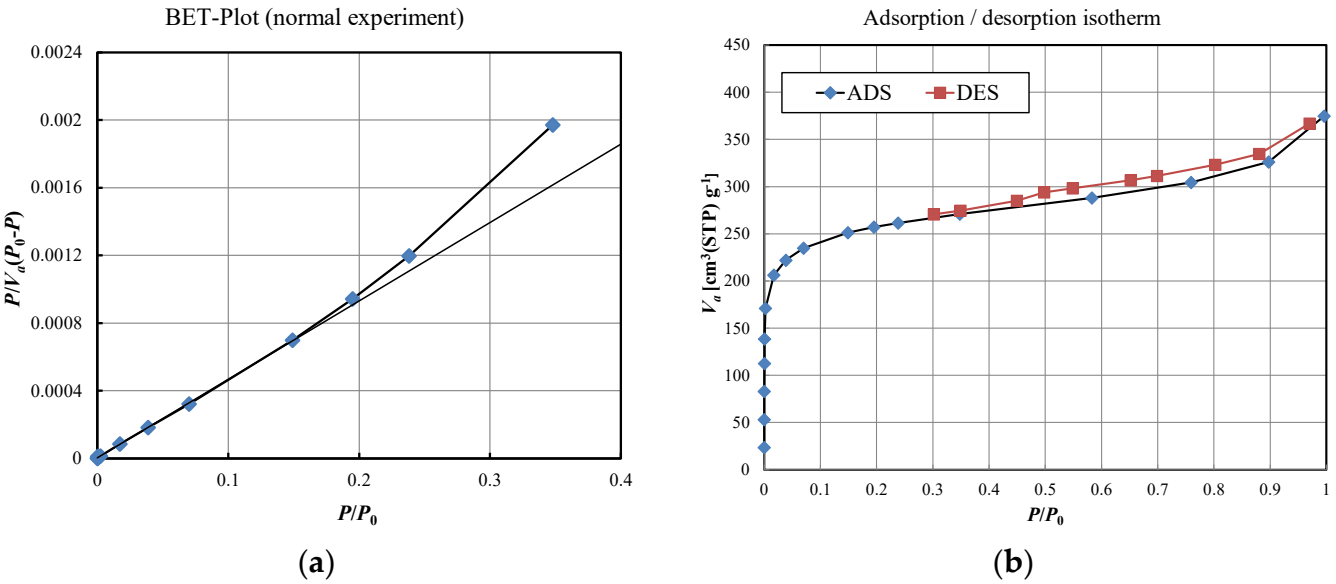

Figure 11. BET plot of (**a**) normal state, (**b**) adsorption and desorption process.

This is explained by determining the adsorption capacity under different relative pressures, which highlights the role of the porosity of the AC in determining the largest value of this capacity, which means the maximum amount of methanol that can be adsorbed by the carbon, and it retains more of it during the adsorption stage.

The DSC test results reveal the thermal behaviour of the AC sample versus temperature, as shown in Figure 12a. The differential scanning curve shows endothermic and exothermic transitions as the temperature increases from 305 to 525 [K]. These critical transitions appear as distinct peaks such 330, 334, and 348 [K], which are reference points for determining the physical properties of the AC sample. Knowing the mass of the sample under study and using the curve data, the specific heat capacity (C_p) of the AC can be calculated through the ratio of heat flow to the change in temperature or the slope of the DSC curve in linear regions, as follows:

$$C_p = \frac{\text{Heat Flow (J)}}{\text{Mass (kg)} \times \Delta T(\ K)} \tag{19}$$

The adsorption content (ΔH_{ads}), or the amount of energy required to adsorb refrigerant vapour onto AC, is expressed by integrating the area under the DSC curve, which represents the amount of heat absorbed or released by the sample when the temperature changes. Thus, the change in heat content or adsorption enthalpy with the sample mass is calculated as follows:

$$\Delta H_{ads} = \frac{\text{Area under the DSC peak (J)}}{\text{Mass of sample (kg)}} \tag{20}$$

The activation energy is related to the reaction rate resulting from the maximum change in temperature that occurs at a large heat flow. It is derived during the adsorption process by using the temperature differences corresponding to the maximum peaks, so it can be calculated from the Arrhenius Equation (4) after analysing the slope of the DSC peak.

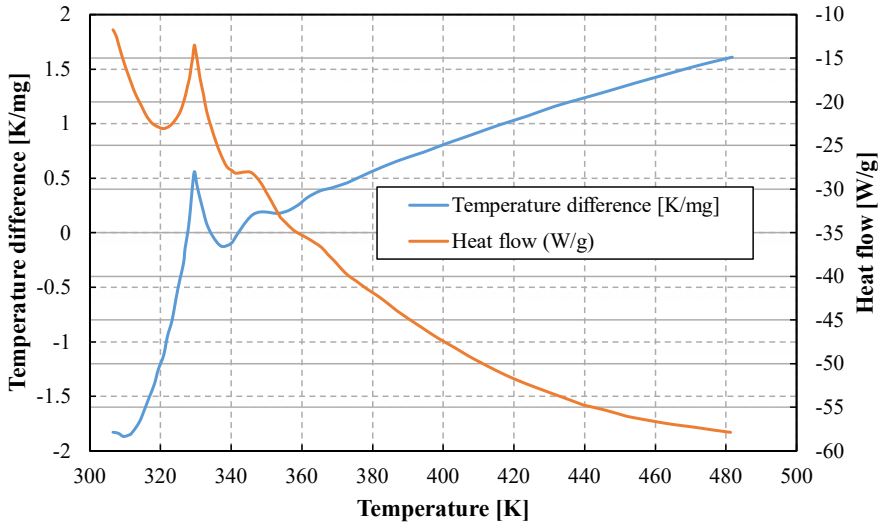

(**a**)

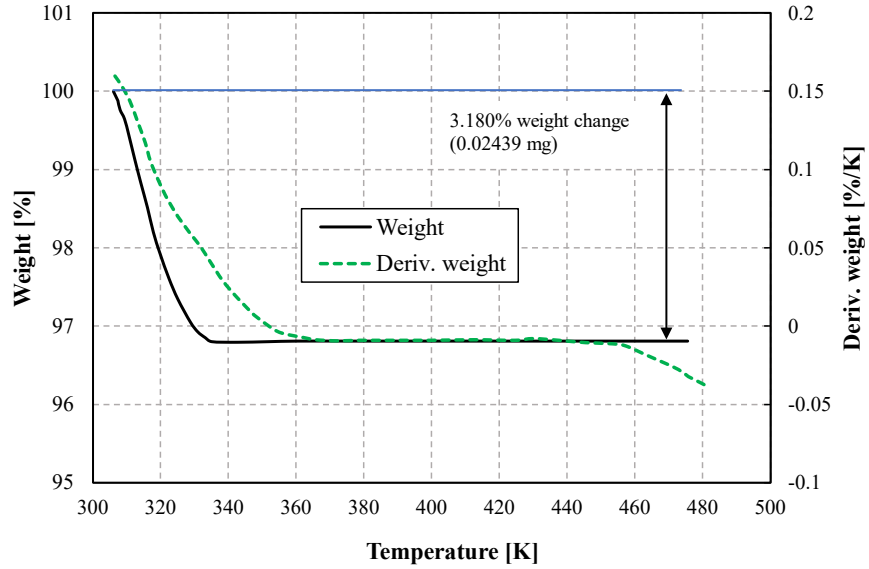

(**b**)

Figure 12. (**a**) DSC test chart; (**b**) TGA test chart with temperature changes in an AC sample.

Figure 12b shows the TGA test results to understand the thermal stability of the AC sample. The graph shows the relative change in weight and the percentage of derived weight as a function of temperature. A significant weight loss of 3.18% is observed, which corresponds to a loss of 0.0243 mg. This decrease is due to moisture loss in the temperature range of 303 to 373 [K]. The maximum weight loss rate is approximately 343 [K], indicating that this type of carbon is thermally stable up to 525 [K]. By knowing the volume of the adsorption bed and the mass of the sample after drying, the total density of the AC can be calculated as follows:

$$\rho_{AC} = \frac{\text{Mass of dry sample (kg)}}{\text{The adsorption bed volume (m}^3\text{)}} \tag{21}$$

All the physical properties of the previous thermal test results are shown in Table 5 for a sample with a grain diameter of d_p and a weight of 0.102 g for the BET test and 0.77 mg for the rest of the tests. These precise measurements of the physical properties are critical for modelling adsorption dynamics, ensuring that the performance of numerical models designed for refrigeration systems can be accurately predicted.

Table 5. Results of (BET-DSC-TGA) tests.

Parameter	ρ_{AC} [kg/m^3]	ΔH_{ads} [kJ/kg]	E_a [J/mol]	x_o [kg/kg]	ε [%]	$C_{p_{AC}}$ [J/(kg.K)]	κ [m^2]	d_p [m]
Test Value (BET-DSC-TGA)	428	1938	4.94×10^4	0.46	0.42	1440	10^{-9}	3×10^{-3}

5.2. Inverse Estimation of the Study Parameters

The termination of the optimisation procedure is carried out in two ways: either by finding the minimum error or by running a certain number of iterations (100) and determining the lowest possible error within them using the labelled error function.

Increasing the population size and iterations enhances the accuracy of the inverse estimation but also requires greater computational resources. By carefully balancing these factors, this study achieved a convergence that was both computationally feasible and highly precise. So, we took the population count $p_n = (25, 50, 100, 150, 200)$ at 100 iterations, and the convergence histories were arranged for comparison. We concluded that at $P_n = 50$, the computation speed is fast enough to be converged; this indicates that the MSE (best fitness function) is less than (10^{-3}) with an acceptable computational cost, as illustrated in Figure 13.

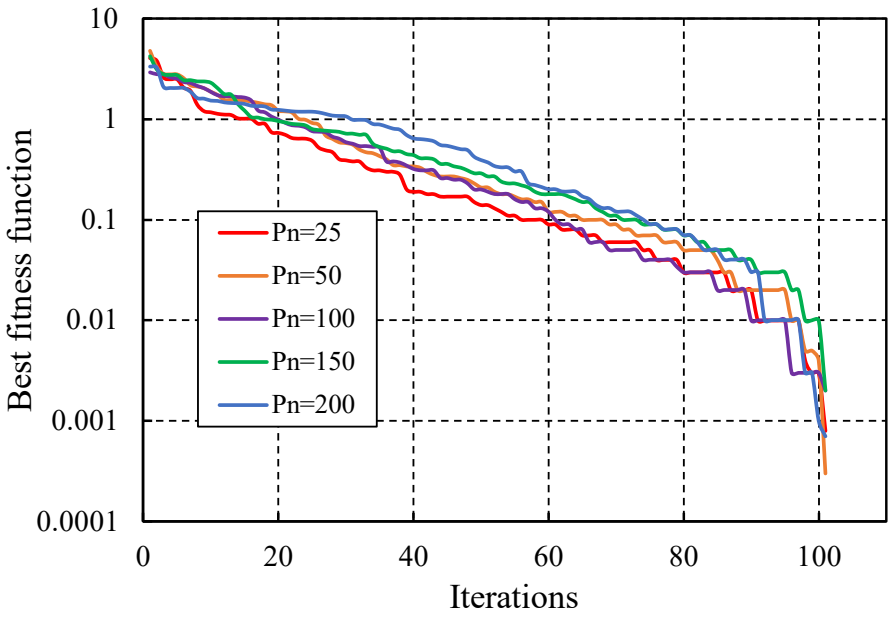

Figure 13. The convergence history chart of the PSO algorithm with different populations.

The unknown parameters which are estimated by this method are the isotherms of the D-A equation constants (n, A), thermal diffusion coefficients (D_m, D_o), external convective heat transfer coefficient (h_{con}), effective heat transfer coefficient of the adsorption bed (λ_{eff}), and contact resistances of the wall (h_{Res}). Table 6 displays all of the significant values, which indicate the previously reported data, the initial estimations, and the fitted optimal values on the experimental data. The reported averages in previous studies form the test limits for the thermal parameters, where an initial guess is given for each parameter and then tested with the rest of all the parameters through the followed algorithm. The optimal values are chosen through the process of fitting the least square error with the experimental temperature changes.

Table 6. Optimal values of the estimation parameters.

Estimated Parameter	n [-]	A [-]	$D_m \times 10^5$ [m^2/s]	$D_o \times 10^4$ [m^2/s]	h_{con} [$W/(m^2.K)$]	λ_{eff} [W/(m.K)]	h_{Res} [$W/(m^2.K)$]	MSE [%]
Optimal Value	0.87	6.7	3.12	3.8	88.21	1.05	264.3	3.51×10^{-4}
Initial Value	1.1	5.7	9	2.54	50	0.99	------	-------
Previous Studies' Average	0.3–1.8	0.3–8	1–9	1–9	10–100	0.2–1.4	50–1000	2–5

In Figure 14, the temperature profiles at the centre of the adsorption bed are presented for two cases when using either the initial or the optimal values, and the results are compared against the experimental data. As a consequence, it is observed that the estimated values could provide a perfect fitting to the experimental data (MSE=3.51×10^{-4}).

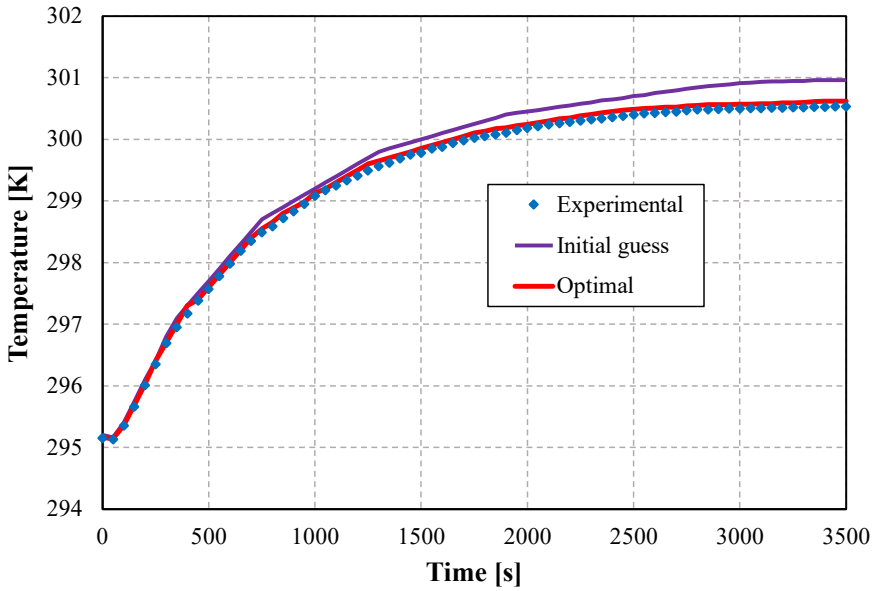

Figure 14. The temperature profiles at the centre of the adsorption bed using the initial and optimal unknown parameters and comparing them against the experimental data.

PSO is characterised by selecting values from the entire searching domain and it does not divide the range into several cells as some algorithms do. Also, the reasonable computational cost associated with the solution's accuracy encourages testing it with more complex adsorption system scenarios, achieving stable operation under various conditions. This confirms that the inverse method is capable of fitting the simulation model to the experimental data to achieve more realistic predictions of system performance. This is due to the direct relationship between the adsorption kinetic equations that parameters were estimated from and the performance indicators of the adsorption cooling system.

5.3. Error and Uncertainty Analysis

Since this study's goal is to idealise adsorption kinetics and estimate thermophysical properties in order to evaluate all of the assumptions made by previous studies, the focus on error analysis is critical. Therefore, the sources of error and uncertainty in this study are analysed systematically, taking into account both experimental measurements and simulation factors. The potential sources of errors in our procedures are measurement

errors arising from experimental equipment, systematic errors arising from uncertainty in numerical analysis, and data processing errors.

Table 1 illustrates the errors in temperature, pressure, and other measurements made by the experiment's measuring devices. These errors cumulatively affect the temperature, pressure, and uptake distribution data used to validate the model and evaluate the physical properties. The BET-DSC-TGA tests for evaluating the physical properties gave a margin error of about (±0.5%) for each, which consequently affected the accuracy of the adsorption capacity, specific heat capacity, adsorption heat, etc.

The primary source of error is evaluated using the MSE, which measures the average of the squares of errors between the simulated and experimental temperature profiles at the centre of the adsorption bed. This can cause a small error after over 100 iterations due to the close linking between MATLAB and COMSOL via the PSO algorithm. The low recurring margin of error around mean values confirms the correct selection of the parameters, as well as the model's ability to represent thermophysical phenomena. To mitigate these errors, we performed a sensitivity analysis, which evaluates how variations in input parameters affect the results using realistic ranges. We then monitored the effect on the error, or the average relative error between the experimental and simulated values, for several tests. This was carried out by repeating the adsorption experiment several times after varying the amount of AC at the same density as the thermal insulator. In addition, the error values in the measuring and data transmission devices were confirmed by comparing them with previous studies that used the same devices for adsorption processes [42].

This approach not only enhances the accuracy of the simulation but also provides a clearer understanding of the physical mechanisms governing the adsorption process, thus providing a more accurate interpretation of the observed discrepancies. The total error strategy was implemented by combining these errors using the root square sum (RSS) method. The following equation shows a breakdown of the estimated errors from different sources [43]:

$$E_{total} = \sqrt{\sum_{i=1}^{5} E^2_{Measuring\ devices} + \sum_{i=1}^{3} E^2_{Laboratory\ tests} + E^2_{Modeling} + E^2_{Data\ processing}} \quad (22)$$

The estimated total error of about 0.87% indicates a realistic range for the study by combining accurate experimental measurements, a robust simulation framework, and comprehensive sensitivity analysis. As a result, this analysis helps to validate the results and provides a clear path for future work to reduce uncertainty.

5.4. Thermodynamic Analysis of the Adsorption Bed

To confirm the validity of the above-estimated parameters, the data can also be fitted for pressure and uptake changes within the adsorption bed, which supports the success of this method. The observed changes in temperature, pressure, and uptake are directly related to the physical mechanisms of mass and heat transfer within the porous structure of AC. This is because the exothermic nature of the adsorption process clearly affects this distribution within the adsorption bed, as shown in Figure 15. At an early stage of the adsorption process (200 s), a thermal wave is observed at the methanol inlet, which expands to take a homogeneous distribution after 3000 s, indicating the dissipation of heat from the interior to the surrounding areas due to adsorption. This is attributed to the effective thermal conductivity of the adsorption bed, whose value plays an important role in the correct temperature distribution.

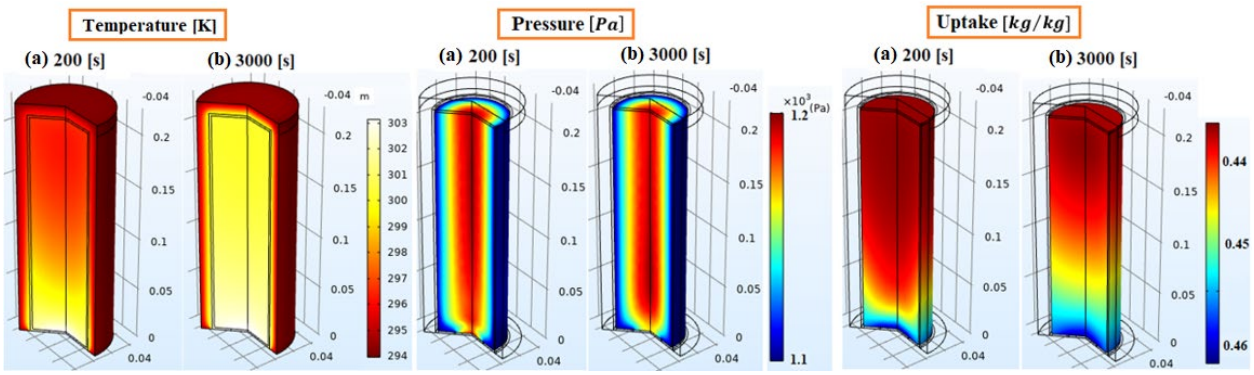

Figure 15. Temperature, pressure, and uptake distribution in the adsorption bed.

The pressure distribution inside the adsorption bed also shows a significant gradient from the inlet to the outlet at the same time, reflecting the initial immersion of methanol vapour into the carbon granules, making the pressure inside the bed more uniform, indicating that the adsorption process has reached a quasi-steady state. The same is true for the uptake distribution, where the adsorption is concentrated near the vapour inlet and becomes more uniform as the methanol spreads and is successfully adsorbed throughout the bed, indicating that the adsorption rate has decreased as the carbon reaches its maximum capacity at time 3000 [s].

The experimental pressure and uptake distribution values during the adsorption process are compared against the numerical outcomes, as exhibited in Figure 16. Pressure readings were taken through the pressure sensor at the inlet of the adsorption bed. The agreement between the numerical and experimental pressure data indicates the model's ability to capture the transient pressure behaviour, which is characterised by accurate measurement during the adsorption process within a very narrow range 1100–1104 [kPa], as shown in Figure 16a, reflecting the correct analysis of adsorption kinetics such as enthalpy and diffusion coefficients.

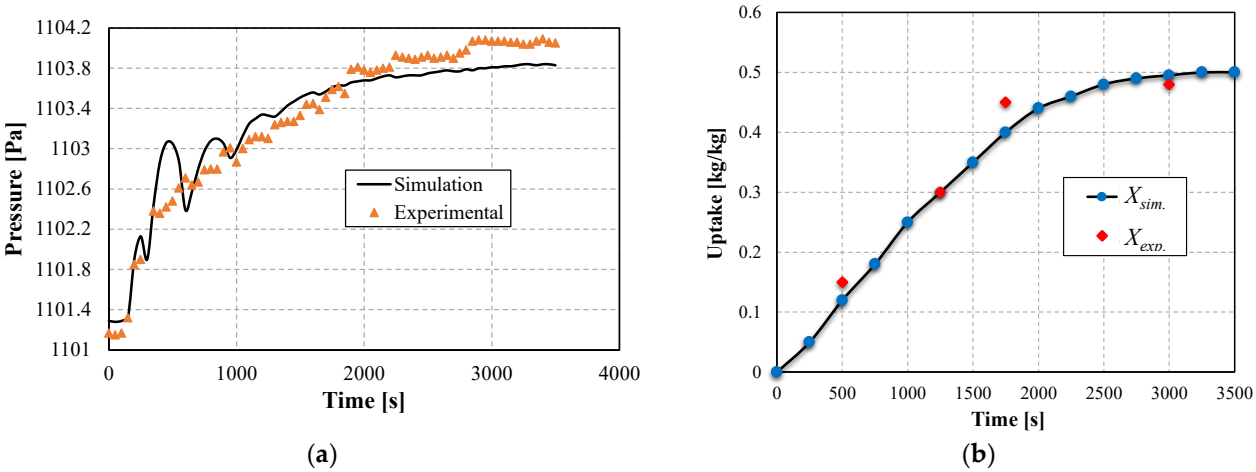

Figure 16. Comparing the experimental and numerical results during the adsorption process using the estimated parameters; (**a**) pressure at the centre of the bed; and (**b**) uptake.

The adsorption results, which measure the amount of methanol adsorbed over time, are demonstrated in Figure 16a and show satisfactory agreement between the experimental and simulation data. This was achieved by weighing the adsorption bed several times over varying times. The fitting process confirms that the estimated adsorption capacity and kinetic parameters effectively describe the system's behaviour. Therefore, the adopted numerical model can be used to explore different design parameters such as bed geom-

etry and composite working pair characteristics, which further enhance the efficiency of adsorption refrigeration cycles.

The relative errors of the pressure and uptake quantities at different time points during the adsorption process are analysed, according to Figure 16b. The pressure and uptake showed the maximum relative error (0.04%, 3.2%), respectively, while the average relative error was (0.01%, 1.2%) for each. It was observed that the increase in the relative error of uptake compared to pressure is due to the difficulty in weighing the adsorption bed during the adsorption process, in addition to the measurement error of the scale. In general, these low relative errors confirm the reliability of the simulation framework in predicting adsorption behaviour, thus affirming the validity of the methodology and the work's results.

6. Conclusions

A method of determining the thermo-physical parameters of adsorption working pairs has come amid continuous growth in recent studies regarding various cooling applications. This trend aims to achieve an accurate thermal analysis of adsorption cooling cycles tailored to operational conditions.

Notably, this work focuses on studies involving granular activated carbon (GAC), where the explicit expression of adsorption equation constants is lacking. This study conducted an inverse parameter estimation process to ascertain the fundamental parameters of the carbon/methanol pair.

A newly developed activated carbon variant (208C) underwent rigorous thermal laboratory tests (BET-DSC-TGA) to determine its thermo-physical properties. The sensitivity analysis of adsorption parameters involved determining coefficients for heat and mass transfer equations based on a thermal analysis of the adsorption process. This was carried out via experimental investigation using a purpose-designed insulated adsorption bed. The experimental results were then simulated using a 3D model in COMSOL Multiphysics software. The integration of the particle swarm optimisation (PSO) algorithm to minimise the mean square error (MSE) in MATLAB software facilitated fitting the experimental results with the numerical model. This integration was facilitated through a live-link system between the two programmes, enabled by a dedicated server. The results were obtained sequentially:

1. The adsorption capacity, porosity, permeability, specific heat capacity, adsorption enthalpy, and activation energy of the activated carbon variant (208C) were determined via thermal tests (BET-DSC-TGA) conducted in a specialised laboratory.
2. The (D-A) equation constants, energy equation parameters' sensitivity (λ_{eff}), and LDF model diffusion coefficients for heat and mass transfer were estimated by fitting the simulation data with the experimental results of temperature changes at the adsorption bed centre.
3. The thermal contact resistance of the insulated adsorption bed wall based on the overall heat transfer coefficient analysis of its configuration was calculated and compared with a non-isolated model according to the previous fitting steps.
4. The optimal values were obtained at the iterations number 100 using different populations ($p_n = 25, 50, 150, 200$), where the best fitness function of results converged to 10^{-4} and $p_n = 50$ could provide acceptable results with appropriate computational costs.
5. After comparing the optimal values with the initial reference values and the experimental results, they were organised into a table, where there was good agreement with the lowest possible error of 3.51×10^{-4}.

6. The thermal analysis of the uptake and pressure distribution within the adsorption bed was repeated with the new estimation values based on a 3D model that simulated the experimental results of the pressure sensor and uptake weights. The accuracy of the results was confirmed by finding the relative error of pressure and uptake changes (1.2%) and then determining the total error of the experimental work and the simulation model (0.87%).

This study demonstrates the efficacy of the inverse method in estimating the parameters of adsorption and kinetic equations. However, to enhance the accuracy and applicability of this approach more broadly, future research should focus on improving this method with other working pairs, performing adsorption process analysis for larger geometry adsorption beds, and developing more accurate optimisation algorithms to dynamically adjust the estimation process based on adsorption time changes and different operating conditions. Detailed sensitivity analyses on the effects of particle size and surface area are also needed to optimise the adsorption capacity. Finally, there is an opportunity to integrate the estimation method with adsorption cooling systems powered by renewable energy, such as solar energy, all of which will ultimately facilitate the optimisation of adsorption systems for industrial applications.

Author Contributions: Conceptualization, M.O. and M.S.; methodology, M.O. and M.S.; software, M.O.; validation, M.O.; formal analysis, M.O., M.S., and M.B.; investigation, M.O., M.S., and M.B.; resources, M.S.; data curation, M.O. and M.S.; writing—original draft preparation, M.O.; writing—review and editing, M.S., and M.B.; visualization, M.O. and M.S.; supervision, M.S., and M.B.; project administration, M.S.; funding acquisition, M.S, and M.B. All authors have read and agreed to the published version of the manuscript.

Funding: This research received no external funding.

Data Availability Statement: No new data where created.

Acknowledgments: The authors would like to thank S. Rahmani and Shimipajoohan Ltd. (No. 3/1, 2nd Alef Alley, Biston Street, Fatemi Square, Tehran, Iran) for their assistance in securing a good type of activated carbon.

Conflicts of Interest: The authors declare that there are no conflicts of interest related to this work.

Nomenclature

C_p	Specific heat capacity [J/kg/K]
D_m	Effective diffusivity [m^2/s]
D_o	Reference diffusivity [m^2/s]
d_p	Particle diameter [m]
E	Error [%]
E_a	Activation energy [J/kg]
h_{Res}	Contact resistances
L	Length of adsorption bed [m]
M	Molar mass [kg/mol]
n, A, D	Dubinin–Astakhov equation coefficient (heterogeneity parameter) [-]
P	Pressure [Pa]
p_n	Population number
R	Universal gas constant [J/(mol.K)]
Rv	Ideal gas constant for water vapour [J/(kg.K)]
r	Radius [m]
T	Temperature [K]
t	Time [s]
V	Velocity vector

v	Velocity of vapour
x	Average adsorbate uptake [kg/kg]
x_o	Maximum adsorption capacity [kg/kg]
Greek symbols	
ΔH	Adsorption enthalpy [kJ/kg]
ε	Porosity [-]
κ	Permeability [m^2]
λ	Heat transfer coefficient [W/m/K]
μ	Dynamic viscosity of refrigerant [Pa.s]
ρ	Density [kg/m^3]
Subscripts	
ads	Adsorption
con	Conductive
eff	Effective
exp	Experimental
eva	Evaporation
in	Inlet
ini	Initial
ins	Insulation
l	Liquid
ove	Overall
meth	Methanol
res	Resistance
s	Solid (adsorbent material)
sat	Saturation conditions
sim	Simulated
st	Stainless steel
Tot	Total
Abbreviations	
AC	Activated carbon
BET	Brunauer–Emmett–Teller test
D-A	Dubinin–Astakhov
DC	Direct current
DSC	Differential scanning calorimetry
FEM	Finite element method
GAC	Granular activated carbon
LDF	Linear driving force
LTNE	Local thermal non-equilibrium
MSE	Mean square method
PSO	Particle swarm optimisation
RMSD	Root mean square deviation
TGA	Thermal gravimetric analysis

References

1. Elsheniti, M.B.; Rezk, A.; Shaaban, M.; Roshdy, M.; Nagib, Y.M.; Elsamni, O.A.; Saha, B.B. Performance of a Solar Adsorption Cooling and Desalination System Using Aluminum Fumarate and Silica Gel. *Appl. Therm. Eng.* **2021**, *194*, 117116. [CrossRef]
2. Ezgi, C. Design and Thermodynamic Analysis of Waste Heat-Driven Zeolite–Water Continuous-Adsorption Refrigeration and Heat Pump System for Ships. *Energies* **2021**, *14*, 699. [CrossRef]
3. Chauhan, P.R.; Kaushik, S.C.; Tyagi, S.K. A Review on Thermal Performance Enhancement of Green Cooling System Using Different Adsorbent/Refrigerant Pairs. *Energy Convers. Manag. X* **2022**, *14*, 100225. [CrossRef]
4. Dias, J.M.S.; Costa, V.A.F. Modeling and Analysis of a Coated Tube Adsorber for Adsorption Heat Pumps. *Energies* **2021**, *14*, 6878. [CrossRef]
5. Mohammed, R.H.; Mesalhy, O.; Elsayed, M.L.; Hou, S.; Su, M.; Chow, L.C. Physical Properties and Adsorption Kinetics of Silica-Gel/Water for Adsorption Chillers. *Appl. Therm. Eng.* **2018**, *137*, 368–376. [CrossRef]

6. Singh, V.K.; Kumar, E.A.; Saha, B.B. Adsorption Isotherms, Kinetics and Thermodynamic Simulation of CO_2-CSAC Pair for Cooling Application. *Energy* **2018**, *160*, 1158–1173. [CrossRef]
7. Khanam, M.; Jribi, S.; Miyazaki, T.; Saha, B.B.; Koyama, S. Numerical Investigation of Small-Scale Adsorption Cooling System Performance Employing Activated Carbon-Ethanol Pair. *Energies* **2018**, *11*, 1499. [CrossRef]
8. Shabir, F.; Sultan, M.; Miyazaki, T.; Saha, B.B.; Askalany, A.; Ali, I.; Zhou, Y.; Ahmad, R.; Shamshiri, R.R. Recent Updates on the Adsorption Capacities of Adsorbent-Adsorbate Pairs for Heat Transformation Applications. *Renew. Sustain. Energy Rev.* **2020**, *119*, 109630. [CrossRef]
9. Hassan, H.Z.; Mohamad, A.A.; Alyousef, Y.; Al-Ansary, H.A. A Review on the Equations of State for the Working Pairs Used in Adsorption Cooling Systems. *Renew. Sustain. Energy Rev.* **2015**, *45*, 600–609. [CrossRef]
10. Çağlar, A.; Yamali, C. Analysis of heat and mass transfer in the adsorbent bed of a thermal wave adsorption cooling cycle. *Comput. Therm. Sci. Int. J.* **2013**, *5*, 97–106. [CrossRef]
11. Shaaban, M.; Elsheniti, M.B.; Rezk, A.; Elhelw, M.; Elsamni, O.A. Performance Investigation of Adsorption Cooling and Desalination Systems Employing Thermally Enhanced Copper Foamed Bed Coated with SAPO-34 and CPO-27(Ni). *Appl. Therm. Eng.* **2022**, *205*, 118056. [CrossRef]
12. Wang, L.W.; Wang, R.Z.; Lu, Z.S.; Chen, C.J.; Wang, K.; Wu, J.Y. The Performance of Two Adsorption Ice Making Test Units Using Activated Carbon and a Carbon Composite as Adsorbents. *Carbon* **2006**, *44*, 2671–2680. [CrossRef]
13. Rupam, T.H.; Islam, M.A.; Pal, A.; Saha, B.B. Adsorption Thermodynamics and Performance Indicators of Selective Adsorbent/Refrigerant Pairs. *Appl. Therm. Eng.* **2020**, *175*, 115361. [CrossRef]
14. Wu, J.W.; Madani, S.H.; Biggs, M.J.; Phillip, P.; Lei, C.; Hu, E.J. Characterizations of Activated Carbon–Methanol Adsorption Pair Including the Heat of Adsorptions. *J. Chem. Eng. Data* **2015**, *60*, 1727–1731. [CrossRef]
15. Yagnamurthy, S.; Rakshit, D.; Jain, S.; Rocky, K.A.; Islam, M.A.; Saha, B.B. Adsorption of Difluoromethane onto Activated Carbon Based Composites: Thermophysical Properties and Adsorption Characterization. *Int. J. Heat Mass Transf.* **2021**, *171*, 121112. [CrossRef]
16. Zhao, Y.; Hu, E.; Blazewicz, A. A Comparison of Three Adsorption Equations and Sensitivity Study of Parameter Uncertainty Effects on Adsorption Refrigeration Thermal Performance Estimation. *Heat Mass Transf.* **2012**, *48*, 217–226. [CrossRef]
17. Rahman, M.M.; Shafiullah, A.Z.; Pal, A.; Islam, M.A.; Jahan, I.; Saha, B.B. Study on Optimum IUPAC Adsorption Isotherm Models Employing Sensitivity of Parameters for Rigorous Adsorption System Performance Evaluation. *Energies* **2021**, *14*, 7478. [CrossRef]
18. Jin, Z.; Tian, B.; Wang, L.; Wang, R. Comparison on Thermal Conductivity and Permeability of Granular and Consolidated Activated Carbon for Refrigeration. *Chin. J. Chem. Eng.* **2013**, *21*, 676–682. [CrossRef]
19. Jegede, O.O.; Critoph, R.E. Extraction of Heat Transfer Parameters in Active Carbon–Ammonia Large Temperature Jump Experiments. *Appl. Therm. Eng.* **2016**, *95*, 499–505. [CrossRef]
20. Khaliji Oskouei, M.; Tamainot-Telto, Z. Investigation of the Heat Transfer Properties of Granular Activated Carbon with R723 for Adsorption Refrigeration and Heat Pump. *Therm. Sci. Eng. Prog.* **2019**, *12*, 1–12. [CrossRef]
21. Azahar, F.H.M.; Mitra, S.; Yabushita, A.; Harata, A.; Saha, B.B.; Thu, K. Improved Model for the Isosteric Heat of Adsorption and Impacts on the Performance of Heat Pump Cycles. *Appl. Therm. Eng.* **2018**, *143*, 688–700. [CrossRef]
22. Zhao, C.; Wang, Y.; Li, M.; Du, W. Heat Transfer Performance Investigation on a Finned Tube Adsorbent Bed with a Compound Parabolic Concentrator (CPC) for Solar Adsorption Refrigeration. *Appl. Therm. Eng.* **2019**, *152*, 391–401. [CrossRef]
23. Elsheniti, M.B.; Eissa, M.S.; Al-Ansary, H.; Orfi, J.; El-Leathy, A.; Elsamni, O. Using a Combination of Activated Carbon and Graphene Nanoparticles in a Consolidated Form for Adsorption Ice Maker: A System-Level Modeling. *Appl. Sci.* **2022**, *12*, 7602. [CrossRef]
24. Albaik, I.; Badawy Elsheniti, M.; Al-Dadah, R.; Mahmoud, S.; Solmaz, İ. Numerical and Experimental Investigation of Multiple Heat Exchanger Modules in Cooling and Desalination Adsorption System Using Metal Organic Framework. *Energy Convers. Manag.* **2022**, *251*, 114934. [CrossRef]
25. Mitra, S.; Muttakin, M.; Thu, K.; Saha, B.B. Study on the Influence of Adsorbent Particle Size and Heat Exchanger Aspect Ratio on Dynamic Adsorption Characteristics. *Appl. Therm. Eng.* **2018**, *133*, 764–773. [CrossRef]
26. Mohammed, R.H.; Mesalhy, O.; Elsayed, M.L.; Chow, L.C. Performance Evaluation of a New Modular Packed Bed for Adsorption Cooling Systems. *Appl. Therm. Eng.* **2018**, *136*, 293–300. [CrossRef]
27. Hadj Ammar, M.A.; Benhaoua, B.; Bouras, F. Thermodynamic Analysis and Performance of an Adsorption Refrigeration System Driven by Solar Collector. *Appl. Therm. Eng.* **2017**, *112*, 1289–1296. [CrossRef]
28. Lowell, S.; Shields, J.E.; Thomas, M.A.; Thommes, M. Surface Area Analysis from the Langmuir and BET Theories. In *Characterization of Porous Solids and Powders: Surface Area, Pore Size and Density*; Lowell, S., Shields, J.E., Thomas, M.A., Thommes, M., Eds.; Particle Technology Series; Springer: Dordrecht, The Netherlands, 2004; pp. 58–81. ISBN 978-1-4020-2303-3.
29. Su, C.-H.; Wu, S.-H.; Shen, S.-J.; Shiue, G.-Y.; Wang, Y.-W.; Shu, C.-M. Thermal Characteristics and Regeneration Analyses of Adsorbents by Differential Scanning Calorimetry and Scanning Electron Microscope. *J. Therm. Anal. Calorim.* **2009**, *96*, 765–769. [CrossRef]

30. Saka, C. BET, TG–DTG, FT-IR, SEM, Iodine Number Analysis and Preparation of Activated Carbon from Acorn Shell by Chemical Activation with $ZnCl_2$. *J. Anal. Appl. Pyrolysis* **2012**, *95*, 21–24. [CrossRef]
31. Yousef, S.; Eimontas, J.; Striūgas, N.; Abdelnaby, M.A. Pyrolysis Kinetic Behaviour and TG-FTIR-GC–MS Analysis of Coronavirus Face Masks. *J. Anal. Appl. Pyrolysis* **2021**, *156*, 105118. [CrossRef]
32. Tamainot-Telto, Z. Novel Method Using Dubinin-Astakhov Theory in Sorption Reactor Design for Refrigeration and Heat Pump Applications. *Appl. Therm. Eng.* **2016**, *107*, 1123–1129. [CrossRef]
33. Çağlar, A. The Effect of Fin Design Parameters on the Heat Transfer Enhancement in the Adsorbent Bed of a Thermal Wave Cycle. *Appl. Therm. Eng.* **2016**, *104*, 386–393. [CrossRef]
34. Yaïci, W.; Entchev, E. Coupled Unsteady Computational Fluid Dynamics with Heat and Mass Transfer Analysis of a Solar/Heat-Powered Adsorption Cooling System for Use in Buildings. *Int. J. Heat Mass Transf.* **2019**, *144*, 118648. [CrossRef]
35. Kumita, M.; Yamawaki, N.; Shinohara, K.; Higashi, H.; Kodama, A.; Kobayashi, N.; Seto, T.; Otani, Y. Methanol Adsorption Behaviors of Compression-Molded Activated Carbon Fiber with PTFE. *Int. J. Refrig.* **2018**, *94*, 127–135. [CrossRef]
36. Li, M.; Zhao, Y.; Long, R.; Liu, Z.; Liu, W. Impacts of Non-Adsorbable Gas on the Adsorption-Based Desalination and Cooling System with Fin Branch Configurations. *Appl. Therm. Eng.* **2023**, *219*, 119565. [CrossRef]
37. Bergman, T.L. *Fundamentals of Heat and Mass Transfer*; John Wiley & Sons: Hoboken, NJ, USA, 2011; ISBN 978-0-470-50197-9.
38. Gediz Ilis, G.; Demir, H.; Mobedi, M.; Baran Saha, B. A New Adsorbent Bed Design: Optimization of Geometric Parameters and Metal Additive for the Performance Improvement. *Appl. Therm. Eng.* **2019**, *162*, 114270. [CrossRef]
39. Pal, A.; Uddin, K.; Thu, K.; Saha, B.B. Activated Carbon and Graphene Nanoplatelets Based Novel Composite for Performance Enhancement of Adsorption Cooling Cycle. *Energy Convers. Manag.* **2019**, *180*, 134–148. [CrossRef]
40. Papazoglou, G.; Biskas, P. Review and Comparison of Genetic Algorithm and Particle Swarm Optimization in the Optimal Power Flow Problem. *Energies* **2023**, *16*, 1152. [CrossRef]
41. Ozana, S.; Pies, M.; Docekal, T. Case Studies on Optimization Problems in MATLAB and COMSOL Multiphysics by Means of the Livelink. *AIP Conf. Proc.* **2016**, *1738*, 370006. [CrossRef]
42. Ghorbani, P.; Siavashi, M. Experimental Performance Analysis of Methanol Adsorption in Granular Activated Carbon Packed Bed through Design of a Double Pipe Heat Exchanger with Longitudinal Fins. *Int. Commun. Heat Mass Transf.* **2024**, *158*, 107938. [CrossRef]
43. Mohammed, R.H.; Mesalhy, O.; Elsayed, M.L.; Chow, L.C. Assessment of Numerical Models in the Evaluation of Adsorption Cooling System Performance. *Int. J. Refrig.* **2019**, *99*, 166–175. [CrossRef]